Vol. 15, No. 2 (2026): 652 - 662 http://dx.doi.org/10.23960/jtepl.v15i2.652-662

JURNAL TEKNIK PERTANIAN LAMPUNG

ISSN 2302-559X (print) / 2549-0818 (online)
Journal homepage : https://jurnal.fp.unila.ac.id/index.php/JTP

Severity Level Classification of Bacterial Leaf Blight Disease (*Xanthomonas oryzae*) in Rice Plants (*Oryza sativa L.*) Based on VARI Image Processing

Rafi Dwi Nugraha[1], Herry Nirwanto[1,✉], Sri Wiyatiningsih[1]

[1] Department of Agrotechnology, Faculty of Agriculture, University of National Development "Veteran" East Java, INDONESIA.

Article History:

Received : 28 November 2023
Revised : 19 May 2024
Accepted : 22 June 2024

Keywords:

Agricultural drones, Digital imagery, Disease detection, Image processing, Vegetation index.

Corresponding Author:
✉ herry_n@upnjatim.ac.id
(Herry Nirwanto)

ABSTRACT

Bacterial leaf blight (BLB) caused by Xanthomonas oryzae is one of the main diseases threatening rice productivity in Indonesia. This study aims to classify the severity of BLB in rice plants more effectively using drone-based image processing technology with the VARI (Visible Atmospherically Resistant Index) vegetation index approach. The study was conducted in Wonoayu Subdistrict, Sidoarjo Regency, covering an area of 17 hectares using a DJI Phantom 4 Pro drone equipped with an RGB camera for image acquisition. The data was then analysed through pre-processing, segmentation using the K-Means Clustering method and edge detection, and classification using the Convolutional Neural Network (CNN) algorithm. The results showed that the CNN classification model was able to identify five levels of attack (healthy, mild, moderate, severe, and dead) with an accuracy of 82.25%, and the classification map was able to distinguish the spatial distribution of the disease in agricultural land. This model also showed better performance than conventional monitoring methods. The use of VARI-based image processing from drones has proven effective as an early disease detection method, providing precise solutions for rice plant health management.

1. INTRODUCTION

Rice (*Oryza sativa L.*) is a strategic commodity that plays a critical role in Indonesia's food security system. Disease outbreaks, particularly bacterial leaf blight (BLB) caused by *Xanthomonas oryzae*, can reduce yields by up to 50% and even cause crop failure if not detected early (Aftab *et al*., 2022). Early identification and classification of disease severity are therefore crucial to prevent productivity losses.

Conventional detection methods are typically based on manual visual inspection, which is subjective and inefficient at a large scale. With the advancement of remote sensing and image analysis technologies, the use of drones (Unmanned Aerial Vehicles/UAVs) have become an effective alternative for crop monitoring due to their high precision, flexibility, and efficiency (Wang *et al*., 2021). UAVs enable rapid, non-destructive, cost-effective, and high-resolution data mining for crop monitoring, phenotyping, and management across extensive agricultural areas (Rexha *et al*., 2026).

The integration of UAV imagery with vegetation indices allows objective and quantitative assessment of crop conditions. One widely used index is the Visible Atmospherically Resistant Index (VARI), which utilizes the visible RGB spectrum. Compared to NDVI, which requires near-infrared (NIR) sensors, RGB-based VARI is more affordable while still showing a strong correlation with vegetation health (Huang *et al*., 2020). revious studies by Kazemi & Ghanbari Parmehr (2023) and Gerardo & de Lima (2023) demonstrated that RGB-based indices, when combined with machine learning algorithms such as Random Forest or CNN, can achieve classification accuracies above 80% in detecting crop health status. This approach is expected to contribute to the development of precision agriculture by providing a fast, accurate, and cost-efficient disease detection system (Ashurov *et al*., 2025; Barbedo, 2019).

Therefore, this study aims to: (1) classify the severity of BLB disease in rice plants based on drone images using VARI index analysis; and (2) evaluate the effectiveness of this method compared to conventional monitoring systems in the field. This study is expected to enrich the literature on the application of remote sensing technology and image analysis in agriculture, particularly in the management of BLB disease in rice crops.

2. MATERIALS AND METHODS

2.1. Location

The research was conducted from February to April 2025 on the land of the Sidomakmur I farmer group, Wonokasian Village, Wonoayu District, Sidoarjo Regency, East Java. The geographical coordinates of the location are Latitude -7.427912° and Longitude 112.659733°. The agricultural land used is intensive land with the Ciherang rice variety.

2.2. Tools and Materials

The tools used include a DJI Phantom 4 Pro drone (RGB camera), laptop (AMD Ryzen 5 processor, NVIDIA GT555m, 16GB RAM), Olympus CX33 microscope, autoclave, laminar air flow, Erlenmeyer flask, Bunsen burner, and software: Python 3.13.5 (VSCode 1.99), library openCV, OS, numpy, tensorflow, scikit-learn, pandas, and matplotlib. The OpenCV library plays a crucial role in reading, processing, and analyzing images, including segmentation, edge detection, and classification. The OS library is used as a module or directory in the Python language. The numpy library is used for numerical calculations in Python code. The TensorFlow library is used to build, train, and run Machine Learning & Deep Learning models. The scikit-learn library is used for feature scaling, such as k-means clustering. The pandas library is used to manipulate the data to be used. The matplotlib library is used to visualize the data to be generated. Biological materials include symptomatic rice leaf samples, *Xanthomonas oryzae* isolates, NA, YDC, and OF media, as well as Gram staining (Crystal Violet, Iodine, Decolorizer, Safranin).

2.3. Research Design

This study used a direct field approach with two observation methods: (1) drone-based for RGB image acquisition and VARI counting; (2) direct visual observation as a conventional method. Sampling was conducted using stratified random sampling based on infection severity zones.

2.4. Preparation

2.4.1. Bacterial Isolation and Identification

Symptomatic rice leaves showing bacterial leaf blight lesions were collected from the field. Leaf segments measuring approximately ±1 cm² were surface-sterilized with 70% ethanol for 30 seconds and rinsed twice with sterile distilled water to remove surface contaminants. The sterilized samples were then placed on Nutrient Agar (NA) medium and incubated at room temperature (28 ± 2 °C) for 24–48 hours. Emerging bacterial colonies exhibiting yellow, mucoid, and convex characteristics typical of *Xanthomonas oryzae* pv. oryzae were selected for further characterization.

The isolated cultures were identified based on morphological and physiological characteristics, including Gram staining, oxidative–fermentative (O/F) tests, and growth observation on yeast dextrose calcium carbonate (YDC) medium, following the standard diagnostic procedures described by Schaad *et al*. (2001) and Singh *et al*. (2015). These methods are widely used to isolate and confirm *X. oryzae* pv. oryzae from infected rice leaves (Adhikari *et al*., 1995).

2.5. Image Acquisition and Processing

2.5.1. Image Acquisition

Plant images are captured using a drone at a height of 7 m above ground level. Images are collected at 90 days after sowing (DAS) during the generative phase. Although *Xanthomonas oryzae* pv. *oryzae* can infect rice during both vegetative and generative growth phases, this study focused on the generative phase (90 days after sowing) because bacterial leaf blight symptoms are more visually pronounced and physiologically significant at this stage.

During the generative phase, lesions typically elongate along the leaf veins, chlorosis intensifies, and disease severity strongly correlates with yield reduction (Aftab *et al*., 2022; Mishra *et al*., 2013). This stage provides higher visual contrast between healthy and infected tissues, improving feature extraction and classification accuracy in RGB-based image analysis.

2.5.2. Preprocessing

RGB images were converted to grayscale, followed by noise removal using Gaussian and Median Filtering, and image resizing for computational efficiency.

2.5.3. Tiling

The Tiling process is performed by dividing the drone-recorded land image into tiles of 128×128 pixels according to the TILE_SIZE parameter. The division is done by calculating the number of rows and columns based on the image dimensions. Next, the image is iterated in rows and columns so that each tile piece can be separated and processed individually.

2.5.4. Classification

The classification model uses a CNN with five severity classes: healthy, mild, moderate, severe, and dead. The model is trained using manually labelled data from visualization and field inspection results.

2.6. Parameters

2.6.1. VARI Image Value Analysis

The VARI value was calculated using the formula:

$$\boldsymbol{VARI} = \frac{G-R}{G+R-B} \tag{1}$$

where G, R, and B are the green, red, and blue pixel values. VARI is correlated with the severity of visual disease to assess the accuracy of the classification model. This formulation was adapted from Gitelson *et al*. (2002) and has been applied in UAV-based vegetation mapping studies such as Gerardo & de Lima (2023) and Huang *et al*. (2018).

2.6.2. Disease Severity

The severity of bacterial leaf blight disease was calculated in two ways depending on the observation method used. For conventional observations (on the ground), it can be calculated using the formula adapted from McKinney (1923):

$$IP = \frac{\sum(n\ x\ v)}{Z\ x\ N} \times 100\% \tag{2}$$

where *IP* is infection intensity (%), *n* is number of infected leaves, *v* is infection category value (0-5), *Z* is the highest infection category value (5), and *N* is number of leaves observed. The damage score values were classified as follows: 0 (no attack), 1 (damage scale 1–20%), 2 (damage scale 21–40%), 3 (damage scale 41–60%), 4 (damage scale 61–80%), and 5 (damage scale over 80%).

This formula is a standard method to quantify disease severity in plant pathology, originally proposed by McKinney (1923) and widely applied for bacterial leaf blight assessment in rice (Adhikari *et al*., 1995). It provides a quantitative estimate of disease progression by integrating both frequency and severity of symptoms on infected leaves. For UAV-based image observations, infection percentage was calculated using a threshold-based approach derived from the Visible Atmospherically Resistant Index (VARI), following Huang *et al*. (2020) and Costa *et al*. (2020):

$$IP = \frac{a<Th}{b} \times 100\% \tag{3}$$

where *a* is the number of VARI pixels, *b* is the total number of pixels, and *Th* is the threshold value. This threshold is determined from the average VARI value of healthy plants in the study area. For example, if healthy plants have an average VARI value of 0.3, then pixels with values below 0.3 are considered an indication of plant stress. This rationale

was used to distinguish healthy vegetation from infected or stressed plants, as lower VARI values indicate reduced greenness due to disease infection (Huang *et al*., 2020). This formula estimates the proportion of canopy pixels exhibiting stress symptoms, as indicated by lower VARI values. A similar threshold-based VARI approach was successfully implemented by Gerardo & de Lima (2023) for assessing rice crop health using UAV RGB imagery. Combining both manual and VARI-based methods allows for accurate cross-validation of disease intensity between field data and image-based classification results.

2.7. Data Analysis

The performance evaluation of the proposed method was conducted by comparing the results of BLB detection obtained from drone-based image processing (CNN + VARI) with those from conventional field monitoring. The evaluation focused on assessing the disease intensity percentage and classification accuracy to determine how effectively the drone-based method represents field-observed conditions. The overall accuracy was calculated by comparing the percentage of infected areas identified by both methods. The results were then interpreted to evaluate the applicability of the CNN + VARI approach for early detection and spatial monitoring of BLB disease in rice fields.

3. RESULTS AND DISCUSSION

This research produces a classification of BLB disease severity in rice plants using drone image data based on the VARI index processed through the CNN model. The results are displayed in the form of bacterial identification results, model validation test results, visualization results of disease distribution maps and RGB histograms, and a comparison table of conventional monitoring methods vs Drone + VARI.

3.1. Results of Identification of Bacteria Causing HDB

Pathogen identification was carried out through three tests: Gram test, Oxidative-Fermentative (O/F) test, and YDC media test. The identification results supported that the causative bacteria was *Xanthomonas oryzae* (Table 1). Gram test results show that the isolate is a Gram negative rod-shaped bacteria. This is in accordance with the general character of *Xanthomonas spp.* as described by Aftab *et al.* (2022). O/F test shows that the isolate is oxidative, indicating the ability of aerobic metabolism. Colonies growing on YDC media appeared bright yellow with a round shape and convex surface, according to the typical morphology of *X. oryzae* according to the classification of plant disease laboratories.

The three tests combined provide strong evidence that the bacterium causing the leaf blight observed in the field is *Xanthomonas oryzae*. This identification reinforces the validity that severity classification through drone imagery is indeed based on the confirmed presence of the target pathogen.

3.2. CNN Model Validation Test

The CNN model trained using the transfer learning approach and the Focal Loss function showed excellent performance. The detailed CNN architecture and image sizes were not explicitly described in this section because the model was developed using a transfer learning approach based on a pre-trained convolutional architecture (e.g., ResNet50), where the core structure is already well-documented in existing literature. The focus of this study was on evaluating the performance and applicability of the CNN + VARI integration for disease severity classification rather than proposing a new CNN design. However, in this research, the input image size was standardized to 224 × 224 pixels, following the common configuration of pre-trained models, to ensure computational efficiency and compatibility with the transfer learning framework.

Based on the training result graph (Figure 1) the accuracy value of the training data increased consistently from about 50% to reach 79% at the 30th epoch, while the validation accuracy even reached 82%. This indicates that the model is able to learn steadily from the training data and also has good generalization ability to unseen data. The loss function for both training and validation data decreased significantly, reaching a value close to 0.05 at the end of training. There were no indications of overfitting, as there was no noticeable difference between the training and validation loss curves. Focal Loss proved to be effective in handling class imbalance in this dataset, especially for minority classes such as mild and moderate illness.

Table 1. Results of bacterial isolate identification tests

Test Type	Observation Result	Interpretation	Image
Gram test	Bacillus-shaped, and red in colour	Gram negative bacteria	 Gram stain results
O/F test	Yellow discolouration of tubes without paraffin	Aerobic bacteria	 Oxidative-Fermentative Results
YDC media test	The growing colonies are bright yellow, round and convex	Colony characteristics of *Xanthomonas sp.*	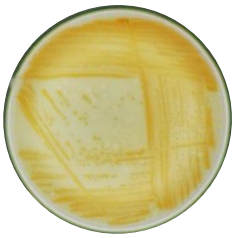 Results of the YDC media test

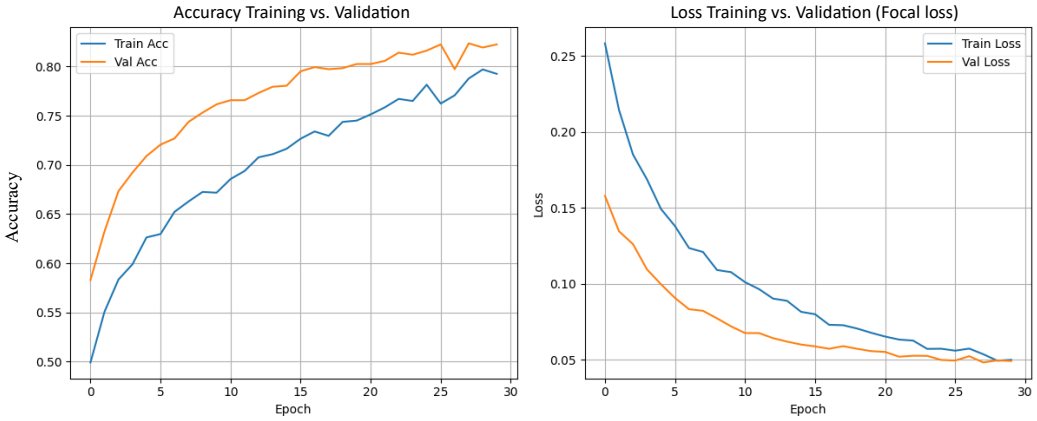

Figure 1. Accuracy (left) and loss (right) of training vs validation

In Table 2, it is known that the model has reached the 30th epoch with a training accuracy of 79.31% with a loss of 0.0501, and a validation accuracy of 82.25% with a loss of 0.0493. The training and validation accuracy values were generated automatically during the CNN training process using the TensorFlow/Keras framework. The accuracy metric represents the ratio of correctly predicted labels to the total number of predictions made by the model during training and validation phases. Although the results are produced programmatically, they are mathematically based on the following general formula (Equation 4):

Table 2. Results of CNN model evaluation with transfer learning and focal loss

Method	Epoch	Total Time (s)	Train Accuracy (%)	Val Accuracy (%)	Train Loss	Val Loss
CNN + Transfer Learning + Focal Loss	30	2.865	79.31	**82.25**	0.0501	0.0493

$$Accuracy = \frac{TP+TN}{TP+TN+FP+FN} \times 100\% \quad (4)$$

where *TP* is true positive (correctly classified infected leaves), *TN* is true negative (correctly classified healthy leaves), *FP* is false positive (healthy leaves misclassified as infected), and *FN* is false negative (infected leaves misclassified as healthy).

The loss value was computed using the Focal Loss function, which modifies the standard Cross-Entropy Loss by reducing the relative loss for well-classified examples and focusing training on difficult or minority classes (Lin *et al*., 2017). This function is defined as the following:

$$FL(p_t) = -\alpha_t(1-p_t)^{\gamma}\log(p_t) \quad (5)$$

where p_t is model's estimated probability for the true class, α_t is class-balancing factor (0–1), and γ is focusing parameter that adjusts the rate at which easy examples are down-weighted.

The training and validation accuracies presented in Table 2 (79.31% and 82.25%) were obtained directly from the model's evaluation metrics at the 30th epoch. These values were automatically tracked and visualized as accuracy and loss curves (Figure 1) using the built-in Keras functions model.fit() and history.history['accuracy']. This analytical approach follows the general evaluation methods for CNN-based image classification described by Ferentinos (2018) and Hasan *et al*. (2020), where model accuracy is continuously computed at each epoch to monitor learning performance and generalization. This performance indicates that the model has successfully adjusted the network weights effectively while maintaining a low error rate (loss) on the test data, thereby concluding that the model is highly suitable for use in the classification inference stage of BLB disease based on VARI drone imagery.

3.3. Visualization of Disease Distribution Map and RGB Histogram

The monitoring results using drone images classified rice plants into five categories based on the severity of the disease: healthy, mildly diseased, moderately diseased, severely diseased, and dead. This classification was analyzed through visual display of the leaves as well as the RGB color histogram and VARI values of each class.

Figure 2 presents RGB intensity histograms corresponding to different levels of rice leaf conditions, ranging from healthy to dead leaves. As shown in the first row of Figure 2, healthy leaves are characterized by a strong dominance of the green (G) channel, indicating high chlorophyll content and active photosynthesis. In contrast, as shown in the second to fourth rows, mildly to severely infected leaves exhibit a gradual increase in the red (R) channel intensity and a reduction in the green channel, reflecting progressive chlorophyll degradation and disease development. Finally, in the last row of Figure 2, dead leaves are dominated by the red channel, with minimal green intensity, indicating the loss of photosynthetic activity.

These observable shifts in RGB distribution across each row of Figure 2 demonstrate that color intensity patterns can effectively represent different disease severity levels. This trend is also consistent with the VARI values obtained, where healthy leaves tend to produce higher (positive) VARI values due to the dominance of the green channel, while infected and dead leaves show decreasing VARI values as the red channel becomes more prominent. As the disease severity increases, the histogram distribution becomes more uneven, reflecting physiological stress and chlorophyll degradation in the leaf tissue.

Furthermore, the classification results based on the VARI method and the CNN model reveal different patterns of disease severity distribution. The VARI approach classifies vegetation based on the relative intensity of the green channel compared to red and blue channels, allowing clear identification of healthy vegetation zones. Meanwhile, the CNN model performs classification by learning complex features from labeled image data using a deep learning approach. A visual comparison indicates that CNN tends to produce more comprehensive classifications; some inconsistencies,

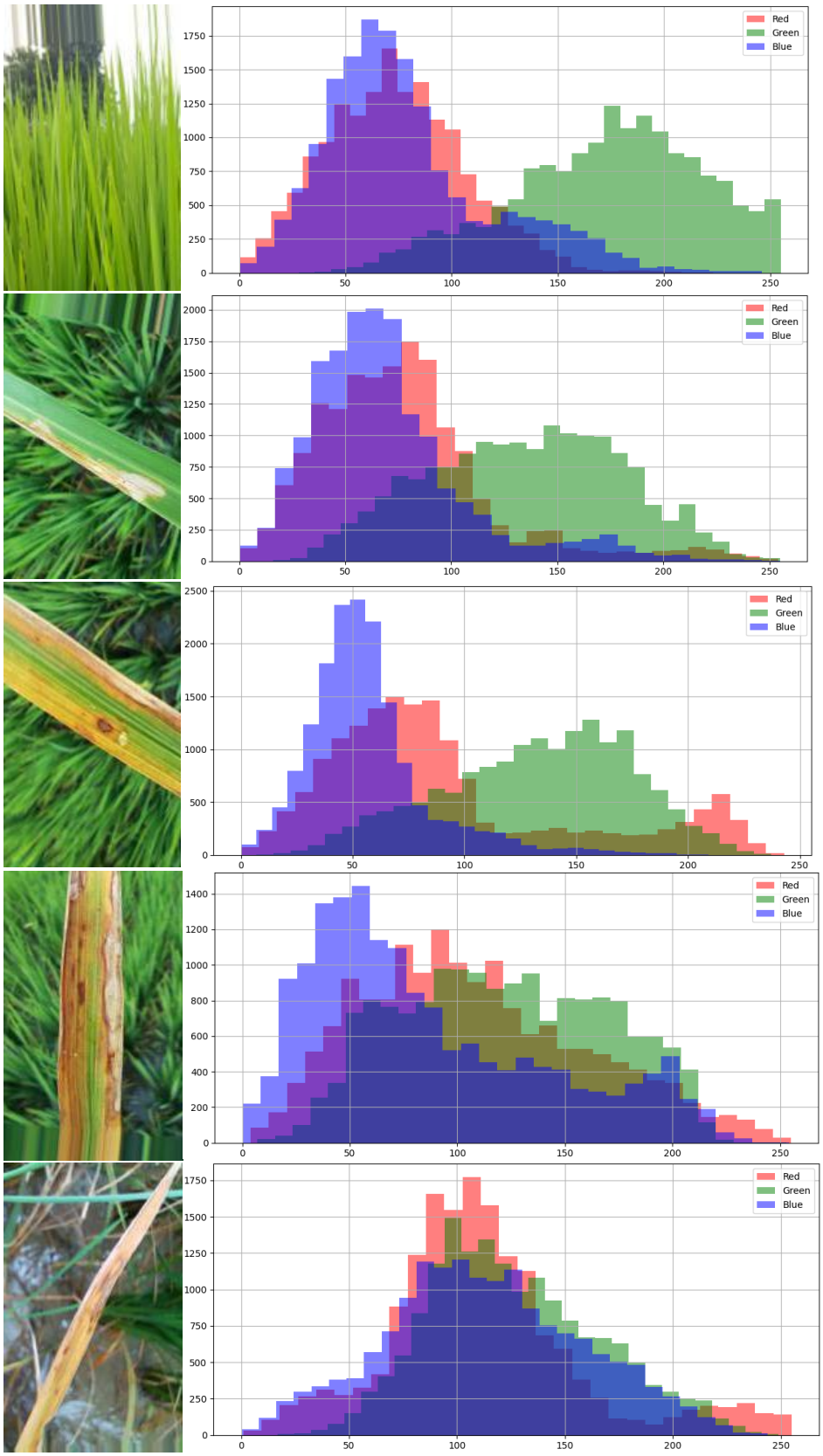

Figure 2. RGB intensity histogram for healthy and infected leaves

however, remain, particularly in distinguishing between mild and moderate disease classes. This suggests that although CNN shows strong predictive capability, further improvement is needed to achieve performance comparable to or better than traditional vegetation index approaches such as VARI.

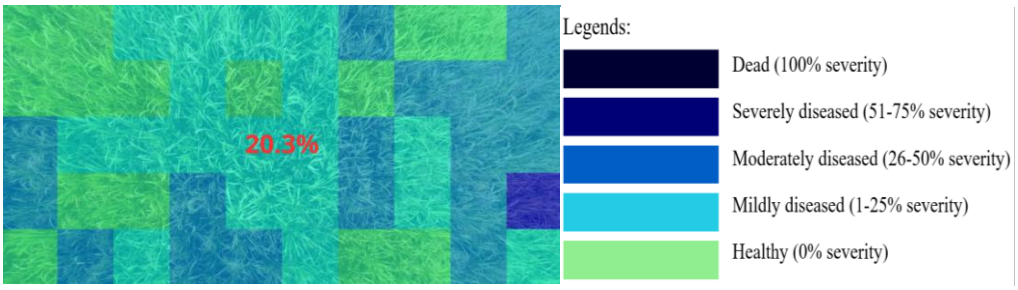

Figure 3. Map of BLB Severity Classification Based on CNN + VARI

Based on the classification map results in Figure 3, it appears that the CNN model produces more detailed classification segmentation compared to the VARI index-based approach. The classification results show a dominance of green areas, both on the map based on the VARI index and the CNN model results. The green color indicates that the plants are in healthy condition with high vegetation index values. There is no significant spread of disease symptoms, and the areas detected as diseased are minimal. Thus, the disease attack intensity is only around 20.3% based on the CNN+VARI model. This finding shows that the system is not only capable of detecting diseases but also provides spatial information for local intervention decision-making. This finding is further supported by findings from Zhu *et al*. (2024), which show that UAV imaging combined with deep learning can identify disease-prone zones with high precision.

Analysis of the RGB color distribution histogram in images for which VARI values have been calculated provides additional quantitative information about plant condition. Figure 4 shows a high dominance of the green (G) color channel, reflecting the higher chlorophyll concentration in healthy rice leaves. This dominance of green reflectance is closely associated with chlorophyll content and photosynthetic efficiency.

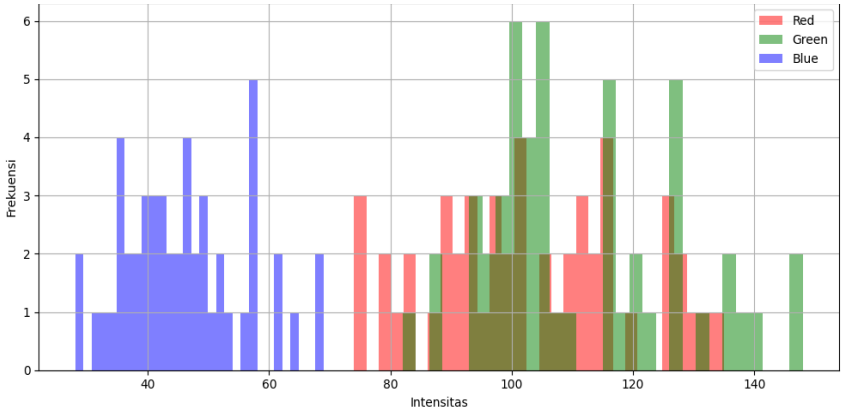

Figure 4. RGB color distribution histogram VARI

Leaves with high chlorophyll concentrations typically absorb light strongly in the blue (B) and red (R) regions while reflecting more in the green (G) region of the visible spectrum. As a result, plants under optimal physiological conditions show higher reflectance in the green channel, which is indicative of robust chlorophyll synthesis and efficient photosynthetic activity (Carter & Knapp, 2001; Gitelson *et al*., 2003; Richardson *et al*., 2002; Sims & Gamon, 2002). Therefore, the observed high green intensity in Figure 4 confirms that the sampled leaves were in a healthy and active photosynthetic state.

3.4. Comparison with Conventional Monitoring

Conventional field monitoring identified a bacterial leaf blight (BLB) intensity of 16% in Plot A. This visual-based approach is limited by subjective interpretation, sampling bias, and restricted spatial coverage. In contrast, the drone-based monitoring approach, using the CNN + VARI model, detected a BLB intensity of 20.3% in the same plot, with a classification accuracy of 78.8% when compared to field observations. The slightly higher intensity value indicates that the drone-based model was able to detect early-stage infection zones that were less visible to the human eye during conventional monitoring.

These results demonstrate that integrating drone imagery with the VARI index and CNN classification provides a more sensitive and spatially comprehensive method for assessing plant health. This finding aligns with the studies of Barbedo (2019), who reported that UAV-based image analysis coupled with deep learning improves the precision of disease mapping in agricultural applications.

Table 3. Comparison of conventional and drone-based monitoring

Monitoring Method	Attack Intensity of BLB (%)
Conventional (manual observation)	16%
Drone + Image Processing (CNN+VARI)	20.3%
Accuracy	78.8%

The infection or attack intensity (*IP*) was calculated following the McKinney (1923) formula, which has been widely adopted in plant pathology studies to quantify disease severity (Equation 2). For the drone-based method, the attack intensity was computed using VARI pixel thresholding, where the percentage of pixels below the healthy vegetation threshold was identified as infected area (Huang *et al*., 2020; Gerardo & de Lima, 2023). The UAV + VARI approach detected an infection intensity of 20.3%, which is slightly higher than the conventional method due to its greater sensitivity to early discoloration and subtle spectral variations in leaf tissue.

This result demonstrates that drone-based RGB imaging combined with VARI analysis provides a more comprehensive and objective assessment of BLB disease distribution across the field, outperforming traditional manual monitoring in both accuracy and spatial coverage. The accuracy value of 78.8% achieved in this study is considered adequate for practical implementation in field-scale disease monitoring. According to Barbedo (2019), classification accuracies above 75% in vegetation image analysis generally indicate strong potential for operational use in precision agriculture. This result also confirms that CNN-based interpretation of VARI indices can effectively support decision-making in plant protection management, enabling early intervention and yield loss prevention.

4. CONCLUSION

The conclusions that can be drawn from this thesis are:

1) The severity of bacterial leaf blight (*Xanthomonas oryzae*.) in rice plants can be identified using drone image analysis based on the VARI vegetation index combined with a transfer learning-based CNN model and the Focal Loss loss function. The developed model can classify five severity levels of the disease with sufficient accuracy, achieving a validation accuracy of 82.25% and a loss value of 0.0493 without overfitting, demonstrating significant potential in supporting the automatic spatial identification of plant diseases.
2) The VARI-based drone image and CNN method was compared with conventional monitoring in detecting disease severity, yielding disease severity levels of 16% (conventional monitoring) and 20.3% (drone monitoring) with comparison accuracy showing 78.8%. This demonstrates that the drone-based VARI and CNN imaging method can cover a wide area and produce more accurate and standardized classifications, making it a potential solution in technology based plant disease monitoring systems.

AUTHOR CONTRIBUTION STATEMENT

Author	C	M	So	Va	Fo	I	R	D	O	E	Vi	Su	P	Fu
RDN	✓	✓	✓	✓	✓	✓	✓	✓	✓	✓	✓		✓	
HN	✓			✓			✓			✓		✓	✓	✓
SW				✓			✓			✓		✓		✓

C: Conceptualization
M: Methodology
So: Software
Va: Validation
Fo: Formal Analysis
I: Investigation
D: Data Curation
R: Resources
O: Writing - Original Draft
E: Writing - Review & Editing
Vi: Visualization
Su: Supervision
Fu: Funding Acquisition
P: Project Administration

REFERENCES

Adhikari, T.B., Cruz, C., Zhang, Q., Nelson, R.J., Skinner, D.Z., Mew, T.W., & Leach, J.E. (1995). Genetic diversity of *Xanthomonas oryzae* pv. *oryzae* in Asia. *Applied and Environmental Microbiology*, ***61***(3), 966–971.

Aftab, U., Ali, S., Ghani, M.U., Sajid, M., Zeshan, M.A., Ahmed, N., & Mahmood, R. (2022). Epidemiological studies of bacterial leaf blight of rice and its management. *Basrah Journal of Agricultural Sciences*, ***35***(1), 106–119. https://doi.org/10.37077/25200860.2022.35.1.09

Ashurov, A.Y., Al-Gaashani, M.S.A.M., Samee, N.A., Alkanhel, R., Atteia, G., Abdallah, H.A., & Muthanna, M.S.A. (2025) Enhancing plant disease detection through deep learning: a Depthwise CNN with squeeze and excitation integration and residual skip connections. *Frontiers in Plant Science*, ***15***, 1505857. https://doi.org/10.3389/fpls.2024.1505857

Barbedo, J.G.A. (2019). Plant disease identification from individual lesions and spots using deep learning. *Biosystems Engineering*, ***180***, 96-107. https://doi.org/10.1016/j.biosystemseng.2019.02.002

Carter, G.A., & Knapp, A.K. (2001). Leaf optical properties in higher plants: linking spectral characteristics to stress and chlorophyll concentration. *American Journal of Botany*, ***88***(4), 677–684. https://doi.org/10.2307/2657068

Costa, L., Nunes, L., & Ampatzidis, Y. (2020). A new visible band index (vNDVI) for estimating NDVI values on RGB images utilizing genetic algorithms. *Computers and Electronics in Agriculture*, ***172***, 105334. https://doi.org/10.1016/j.compag.2020.105334

Ferentinos, K.P. (2018). Deep learning models for plant disease detection and diagnosis. *Computers and Electronics in Agriculture*, ***145***, 311–318. https://doi.org/10.1016/j.compag.2018.01.009

Gerardo, R., & de Lima, I.P. (2023). Applying RGB-based vegetation indices obtained from UAS imagery for monitoring the rice crop at the field scale: A case study in Portugal. *Agriculture*, ***13***(10), 1916. https://doi.org/10.3390/agriculture13101916

Gitelson, A.A., Kaufman, Y.J., Stark, R., & Rundquist, D. (2002). Novel algorithms for remote estimation of vegetation fraction. *Remote Sensing of Environment*, ***80***(1), 76–87. https://doi.org/10.1016/S0034-4257(01)00289-9

Hasan, R.I., Yusuf, S.M., & Alzubaidi, L. (2020). Review of the state of the art of deep learning for plant diseases: A broad analysis and discussion. *Plants*, ***9***(10), 1302. https://doi.org/10.3390/plants9101302

Huang, B., Reichman, D., Collins, L.M., Bradbury, K., & Malof, J.M. (2019). Tiling and stitching segmentation output for remote sensing: Basic challenges and recommendations. *arXiv:1805.12219*. https://arxiv.org/abs/1805.12219

Kazemi, F., & Parmehr, E.G. (2023). Evaluation of RGB vegetation indices derived from UAV images for rice crop growth monitoring. *ISPRS Annals of the Photogrammetry, Remote Sensing and Spatial Information Sciences*, *X-4/W1-2022*, 385–390. https://doi.org/10.5194/isprs-annals-X-4-W1-2022-385-2023

Lin, T.-Y., Goyal, P., Girshick, R., He, K., & Dollár, P. (2017). Focal loss for dense object detection. *Proceedings of the IEEE International Conference on Computer Vision (ICCV)*, 2980–2988. https://doi.org/10.1109/ICCV.2017.324

McKinney, H.H. (1923). Influence of soil temperature and moisture on infection of wheat seedlings by *Helminthosporium sativum*. *Journal of Agricultural Research*, ***26***(5), 195–217.

Mishra, D., Vishnupriya, M.R., Anil, M.G., Konda, K., Raj, Y., & Sonti, R.V. (2013). Pathotype and genetic diversity amongst Indian isolates of *Xanthomonas oryzae* pv. oryzae. *PLoS ONE*, ***8***(11), e81996. https://doi.org/10.1371/journal.pone.0081996

Rexha, G., Papadhopulli, I., Biberaj, A., Agastra, E., Sheme, E., & Meçe, E. (2026). A UAV-based multisensor framework for legal industrial Cannabis monitoring and open-access dataset development. Data in Brief, ***65***, 112463. https://doi.org/10.1016/j.dib.2026.112463

Richardson, A.D., Duigan, S.P., & Berlyn, G.P. (2002). An evaluation of noninvasive methods to estimate foliar chlorophyll content. *New Phytologist*, ***153***(1), 185–194. https://doi.org/10.1046/j.0028-646X.2001.00289.x

Schaad, N.W., Jones, J.B., & Chun, W. (2001). Laboratory Guide for Identification of Plant Pathogenic Bacteria (3rd ed.). American Phytopathological Society Press, St. Paul, MN, USA. ISBN 089054263

Sims, D.A., & Gamon, J.A. (2002). Relationships between leaf pigment content and spectral reflectance across a wide range of species, leaf structures and developmental stages. *Remote Sensing of Environment*, ***81***(2–3), 337–354. https://doi.org/10.1016/S0034-4257(02)00010-X

Singh, D., Sinha, S., & Singh, R. P. (2015). Detection of *Xanthomonas oryzae* pv. oryzae from seeds and leaves of rice using hrp gene based BIO-PCR marker. *Indian Journal of Agricultural Sciences*, 85(4), 519–524. https://doi.org/10.56093/ijas.v85i4. 47932

Wang, T., Liu, Y., Wang, M., Fan, Q., Tian, H., Qiao, X., & Li, Y. (2021). Applications of UAS in crop biomass monitoring: A review. *Frontiers in Plant Science*, ***12***, 616689. https://doi.org/10.3389/fpls.2021.616689

Zhu, H., Lin, C., Liu, G., Wang, D., Qin, S., Li, A., Xu, J-L., & He, Y. (2024). Intelligent agriculture: deep learning in UAV-based remote sensing imagery for crop diseases and pests detection. *Frontiers in Plant Science*. ***15***, 1435016. https://doi.org/10.3389/fpls.2024.1435016